Applications of Polymer, Composite, and Coating Materials

Thiol-ene click synthesis of phenylboronic acid-functionalized covalent organic framework for selective catechol removal from aqueous medium

Shi-Lei Ji, Hai-Long Qian, Cheng-Xiong Yang, Xu Zhao, and Xiu-Ping Yan

ACS Appl. Mater. Interfaces, **Just Accepted Manuscript** • DOI: 10.1021/acsami.9b17324 • Publication Date (Web): 18 Nov 2019

Thiol-Ene Click Synthesis of Phenylboronic Acid-Functionalized Covalent Organic Framework for Selective Catechol Removal from Aqueous Medium

Shi-Lei Ji[†], Hai-Long Qian[‡,§], Cheng-Xiong Yang[†], Xu Zhao[‡,§] and Xiu-Ping Yan*[,‡,§]

[†]College of Chemistry, Research Center for Analytical Sciences, Tianjin Key Laboratory of Molecular Recognition and Biosensing, Nankai University, Tianjin 300071, China

[‡]State Key Laboratory of Food Science and Technology and [§]Institute of Analytical Food Safety, School of Food Science and Technology, Jiangnan University, Wuxi 214122, China

ABSTRACT: We report a thiol-ene click strategy for the preparation of a novel phenylboronic acid-functionalized covalent organic framework (COF) for selective removal of catechol in aqueous solution. Vinyl-functionalized 2,5-diallyloxyterephthalaldehyde (Da-V) was prepared as a building ligand. Da-V was then condensed with 1,3,5-tris(4-aminophenyl)benzene (Tab) to give a vinyl-functionalized COF DhaTab-V. Subsequently, 4-mercaptophenylboronic acid (4-MPBA) was covalently linked on DhaTab-V via thiol-ene click reaction to give phenylboronic acid-functionalized COF DhaTab-PBA. The adsorption isotherms, energetics and kinetics, and reusability of DhaTab-PBA for the adsorption and removal of catechol from aqueous solution were investigated in detail. This phenylboronic acid-functionalized COF is promising as sorbent for selective removal of catechol from aqueous medium with large adsorption capacity and good reusability.

KEYWORDS: thiol-ene click strategy, covalent organic framework, phenylboronic acid, catechol removal, aqueous medium

1. INTRODUCTION

The wide use of catechol as chemical intermediates in industry causes potential environmental risks due to its high toxicity, carcinogenicity, high oxygen demand and low biodegradability.[1-3] Therefore, the removal of catechol from the polluted aqueous environment is of great importance for environmental remediation.[4,5] Up to date, quite a few techniques, such as adsorption,[6,7] electrochemical treatment[8] and chemical decomposition,[9] have been developed for removing catechol from aqueous environment. Adsorption is a frequently used manner in virtue of its features of high efficiency and easy operation.[5] Many sorbents such as activated carbon,[10] resin,[7] and montmorillonite,[11] have been used to remove catechol. However, there are still several limitations with these sorbents such as poor selectivity and low reusability.[12,13] Hence, the development of efficient and reusable sorbent is of great significance for the removal of catechol.[14-17]

Covalent organic framework (COF), a rising type of crystalline porous polymers, has many desirable features, such as low mass density, regular pore structure, high surface area, facilely tailored functionality, and the like.[18] For these reasons, COF has received great attention in diverse fields, such as separation,[19-23] catalysis,[24-26] gas storage[27-29] and optoelectronics.[30-32] Despite COF has been applied for the adsorption of chemical pollutants, previous COF-based adsorption processes are mainly on the basis of hydrophobic interaction and π-π stacking, and usually lack specificity.[33,34]

Introducing appropriate recognition moieties to COF is essential for improving adsorption specificity.[35-38] Boronic acid moiety enables covalent binding of cis-diols molecules to form five/six-membered cyclic esters.[39-41] Therefore, the introduction of boronic acid moiety to COF to develop functionalized sorbent is of great significance to enhance the ability for specific

recognition of cis-diols molecules.[42] Thiol-ene click strategy has been verified to be a feasible way to synthesize functionalized COF for diverse applications due to its high efficiency and selectivity.[37,41] For examples, thiol grafted imine-based and amino-modified COF have been synthesized via the thiol-ene click strategy for selective adsorption of heavy metal ions and carboxylic acid pesticides.[37,41]

Herein, we report a thiol-ene click approach for the fabrication of a novel phenylboronic acid-functionalized COF for selective removal of catechol from aqueous solution. Vinyl-containing ligand 2,5-diallyloxyterephthalaldehyde (Da-V) and 1,3,5-tris(4-aminophenyl)benzene (Tab) are used as building ligands to prepare a vinyl-containing COF DhaTab-V. Subsequent thiol-ene click reaction of the prepared DhaTab-V with 4-mercaptophenylboronic acid (4-MPBA) gives phenylboronic acid-functionalized COF DhaTab-PBA with high adsorption capacity, and good adsorption selectivity and reusability for the removal of catechol from aqueous medium.

2. EXPERIMENTAL SECTION

2.1. Chemicals and Materials. All of above-mentioned reagents and materials were at least analytical grade. 1,3,5-Tris(4-aminophenyl)benzene (Tab), 2,5-dihydroxyterephthalaldehyde (Da) were supplied by Bide Pharmatech Ltd. (Shanghai, China). Acetonitrile, ethanol, *N*,*N*'-dimethylformamide (DMF), tetrahydrofuran (THF), methanol and acetone were provided by Sinopharm Chemical Reagent Co. Ltd. (Shanghai, China). Allyl bromide, *o*-dichlorobenzene (*o*-DCB), *n*-butyl alcohol (*n*-BuOH) and 4-mercaptophenylboronic acid (4-MPBA) were given by Macklin Biochemical Co. Ltd. (Shanghai, China). Catechol, resorcinol, hydroquinone, phenol and azodiisobutyronitrile (AIBN) were provided by Aladdin Chemistry Co. Ltd. (Shanghai, China).

2.2. Instrumentation. Powder X-ray diffraction (PXRD) patterns, thermogravimetric curves, Fourier transform infrared (FT-IR) spectra, nitrogen adsorption-desorption isotherms and Zeta potential data were acquired using the apparatuses described in ref. 43. ^{1}H nuclear magnetic resonance (NMR) analysis was done on a NMR spectrometer at 400 MHz ADVANCE III HD (Bruker, Switzerland). X-ray photoelectron spectra (XPS) were recorded on an Axis supra spectrometer with monochromatized $Al_{K\alpha}$ radiation ($h\nu$ = 1486.6 eV, 225 W) as X-ray source (Kratos, MA, UK). Transmission electron microscopy (TEM) and scanning electron microscope (SEM) images were obtained using the apparatuses described in ref. 27. UV-vis absorption analysis was done on a UV-3600PLUS220/230VC spectrophotometer (Shimadzu, Japan).

Chromatographic measurements were carried out on Waters alliance 2695 HPLC with 2998 PDA detector (Waters, USA) using methanol/0.2% acetic acid (5:5, v/v) as the mobile phase at a flow rate of 0.9 mL min^{-1}. Chromatographic signals were monitored at 277 nm.

2.3. Synthesis of ligand Da-V. Da (0.26 g, 1.56 mmol) and potassium carbonate (1.80 g, 13.02 mmol) were dispersed in 15 mL DMF. Then, allyl bromide (0.74 mL, 8.56 mmol) was dropwise added into the mixture with stirring. The mixture was heated to 70 ^{o}C, stirred for 12 h, and cooled down to room temperature. To the mixture, an appropriate volume of water was added to dissolve potassium carbonate. The resulting product was extracted with ethyl acetate (3 × 10 mL). The collected organic extract was dried with anhydrous magnesium sulfate to remove residual water and condensed on a rotary evaporator. The obtained crude product was purified via recrystallization with a small volume of acetonitrile. The final product Da-V was yellow-green (0.33 g, 86.2%). ^{1}H NMR (400 MHz, $CDCl_3$, 298 K, TMS, ppm): δ 0.5 (s, 1H, C*H*O), 7.45 (s, 2H, Ar*H*), 6.11-6.02 (m, 2H, C*H*), 5.45 (ddd, *J* = 17.2, 2.9, 1.5 Hz, 2H, CH_2), 5.34 (ddd, *J* = 10.5, 2.6, 1.3 Hz, 2H, CH_2), 4.67 (dt, *J* = 5.2, 1.5 Hz, 4H, OCH_2).

2.4. Synthesis of DhaTab-V. Tab (56.20 mg, 0.16 mmol) and Da-V (59.04 mg, 0.24 mmol) were dispersed into a binary solvent of *o*-DCB (3 mL) and *n*-BuOH (3 mL) in a Schlenk tube (35 mL, o.d. = 26, length = 125 mm) under 5-min ultrasonication. Then, acetic acid (6 M, 0.60 mL) was added to the mixture. The mixture was sonicated for 3 min, frozen under liquid nitrogen bath, and degassed with pump. After the tube was sealed with a screw cap, the mixture was heated at 120 ^{o}C for 3 days. The resulting precipitate was collected via centrifugation and washed with DMF and THF for three times. The product was purified with fresh THF and dried at 50 ^{o}C for 24 h under vacuum to afford DhaTab-V (90.30 mg, 84.7%).

2.5. Synthesis of DhaTab-PBA. DhaTab-V (20 mg), 4-MPBA (40 mg, 0.26 mmol) and AIBN (2 mg, 0.012 mmol) were dispersed into 10 mL THF in a flask (50 mL). The mixture was sonicated, degassed and heated at 65 ^{o}C under N_2 for 24 h. The resulting precipitate was collected via centrifugation, washed with DMF and THF, purified with fresh acetone, and dried at 50 ^{o}C under vacuum for 24 h to afford DhaTab-PBA (17.10 mg, 85.5%).

2.6. Adsorption experiments. All of catechol standard solutions used in adsorption experiments except in pH effect study were prepared in phosphate buffer solution (PBS, 10 mmol L^{-1}, pH 8) for optimal adsorption of catechol. To study adsorption kinetics, 0.5 mg DhaTab-PBA and 2 mL standard catechol solution at certain initial concentration were added in a centrifugal tube (5 mL). After mechanical shaking (120 rpm) for a certain time in the range of 0-300 min at room temperature, the mixture was centrifuged to collect the supernatant for UV-vis spectrophotometric determination of residual catechol in solution.

To evaluate adsorption isotherm and thermodynamics, 0.5 mg DhaTab-PBA and 2 mL catechol standard solution at certain initial concentration were added in a centrifugal tube (5 mL) at a fixed temperature in the range of 298-328K for 60 min. Then, the mixture was centrifuged to

collect the supernatant for UV-vis spectrophotometric determination of residual catechol in solution.

To test the effect of pH, the pH of the aqueous standard catechol solution was adjusted to 3-10 with 1 mol L^{-1} HCl and NaOH solution. To examine the effect of ionic strength, the concentration of NaCl in the catechol standard solution was changed.

3. RESULTS AND DISCUSSION

3.1. Synthesis and characterization of DhaTab-PBA. Figure 1 illustrates the design and synthesis of DhaTab-PBA. In view of the large pore width (3.7 nm) of COF DhaTab prepared from Da and Tab,[21] we chose DhaTab as the framework for further functionalization. We started with the synthesis of the vinyl functionalized ligand Da-V from Da and allyl bromide via nucleophilic substitution reaction. The vinyl-functionalized COF (DhaTab-V) was then prepared via the condensation of Da-V and Tab with a solvothermal method. Finally, 4-MPBA was introduced to fabricate the phenylboronic acid-functionalized COF (DhaTab-PBA) via thiol-ene click reaction.

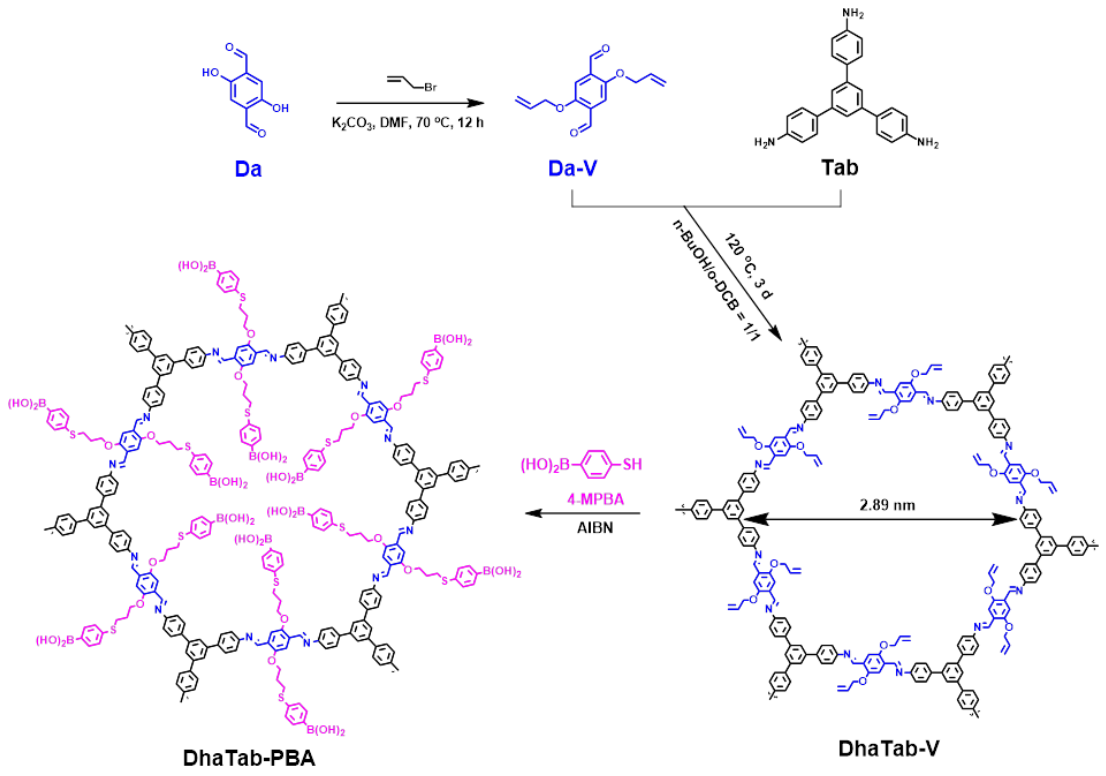

Figure 1. Illustration for the preparation of DhaTab-V via the condensation of Tab and Da-V and DhaTab-PBA via thiol-ene click reaction.

The incorporation of functional moiety on the pore surface via post-synthetic strategy inevitably affects the properties of COF, such as crystallinity, porosity and surface area.[44] Therefore, in the post-synthetic approach, a crucial balance between porosity and functionalization should be established to realize optimal experimental effects. Herein, we investigated different feed amounts of 4-MPBA on the adsorption of catechol on the phenylboronic acid-functionalized COF. The results show that DhaTab-PBA prepared from 0.26 mmol 4-MPBA and 20 mg DhaTab-V gives optimal adsorption capacity for catechol (Table S1).

PXRD experiment and Pawley refinement were carried out to reveal the crystal structures of DhaTab-V and DhaTab-PBA. The two peaks at 2.8° and 5.6° for DhaTab-V and its structure are in good agreement with an eclipsed AA model with the unit cell parameters of a = 36.2658 Å, b = 38.1059 Å, c = 3.8930 Å, α = β = 90° and γ = 120° (Figure 2a and Table S2). There is no great

difference between the experimental PXRD pattern and the refined eclipsed AA model PXRD pattern with factors of R_{wp} = 6.76%, R_{wp} (w/o bck) = 14.68% and R_p = 5.01% (Figure S1). The incorporation of phenylboronic acid to COF resulted in a minor loss of crystallinity compared with DhaTab-V (Figure 2a).

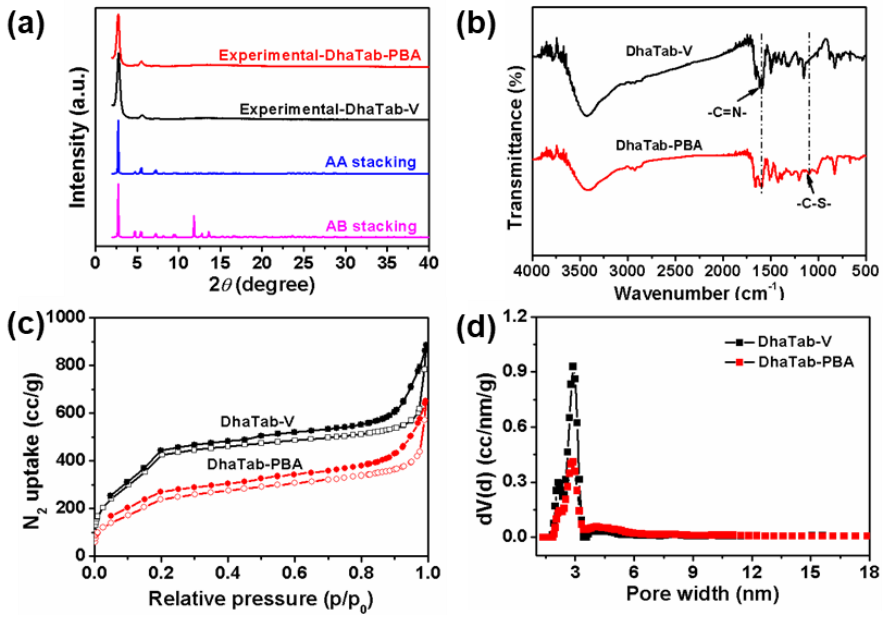

Figure 2. (a) PXRD patterns: experimental pattern of DhaTab-PBA (red line), experimental pattern of DhaTab-V (black line), simulated pattern of DhaTab-V for AA eclipsed model (blue line) and simulated pattern of DhaTab-V for AB eclipsed model (magenta line). (b) FT-IR spectra of DhaTab-V and DhaTab-PBA. (c) Nitrogen adsorption−desorption isotherms of DhaTab-V and DhaTab-PBA. (d) Pore size distribution of DhaTab-V and DhaTab-PBA.

The typical -OH stretching band (3280 cm^{-1}) of Da disappeared but the C=O stretching peak (1670 cm^{-1}) remained in the FT-IR spectra of Da-V (Figure S2a). The C=C stretching band of Da-V was not observed due to an overlap between C=C stretching (1695-1630 cm^{-1}) and C=O stretching (1755-1665 cm^{-1}) bands. However, new bands for C-O stretching (1210 cm^{-1}) and C-H stretching (1380 cm^{-1} and 1423 cm^{-1} from vinyl) appeared in the FT-IR spectra of Da-V (Figure

S2a). Meanwhile, the proton of C=C was verified by ^{1}H NMR analysis (Figure S3). The above results show the successful vinyl modification of Da.

The FT-IR spectra of DhaTab-V show the appearance of new band for C=N stretching (1605 cm^{-1}), the lack of N-H stretching band (3350-3450 cm^{-1}) of Tab, and the significant attenuation of the C=O stretching band (1670 cm^{-1}) of Da-V (Figure S2b), indicating the covalent framework formation of DhaTab-V. The weak C-S stretching band (1092 cm^{-1}) in the FT-IR spectra of DhaTab-PBA was due to the modification of 4-MPBA (Figure 2b).

The sulfur signal at 163.4 eV in the XPS spectra of DhaTab-PBA can be attributed to organosulfur compounds (Figure 3a).[45,46] The appearance of sulfur element in DhaTab-PBA composition also results from the modification of 4-MPBA (Table S3). With the theoretical calculation, XPS and elemental analysis (Figures 3 and S4), the percentages of 4-MPBA modified on COF were determined to be 18.8% to 21.9% of theoretical amount.

The introduction of phenylboronic acid moiety on COF resulted in no obvious change in the morphology of DhaTab-V (Figure S5), but significant decrease in the Brunauer-Emmett-Teller (BET) surface areas from 1032.5 $m^2 g^{-1}$ (DhaTab-V) to 621.5 $m^2 g^{-1}$ (DhaTab-PBA) (Figure 2c). Meanwhile, phenylboronic acid modification also made the total pore volume decrease from 0.88 $cm^3 g^{-1}$ (DhaTab-V) to 0.62 $cm^3 g^{-1}$ (DhaTab-PBA) (Figure 2d).

The fabricated DhaTab-V and DhaTab-PBA are comparatively stable up to 300 ^{o}C (Figure S6). Meanwhile, DhaTab-PBA is also stable in water/PBS (10 mM, pH 8) (Figure S7). Compared with DhaTab-V, DhaTab-PBA carries more negative charge due to the incorporation of boronic acid moiety (Figure S8).

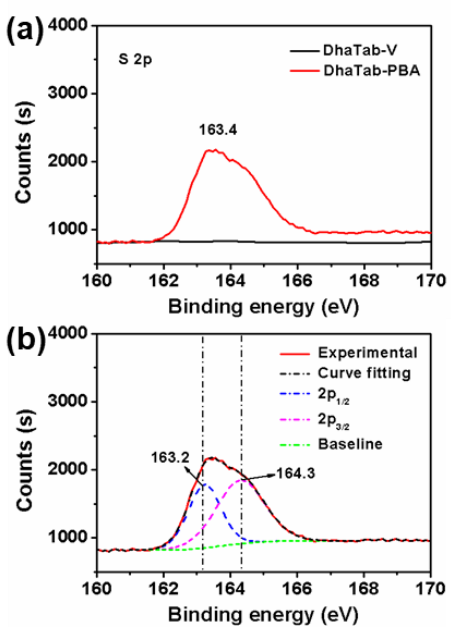

Figure 3. (a) S 2p XPS spectra of DhaTab-V and DhaTab-PBA. (b) S 2p XPS spectra of DhaTab-PBA. Solid curves: the experimental spectra, and dotted curves: the fitting data.

3.2. Adsorption kinetics for catechol. To evaluate the kinetics for the adsorption of catechol on DhaTab-PBA, the time-dependent adsorption capacity (Q_t) was obtained at an initial catechol solution of 0.025, 0.050 and 0.075 mg mL^{-1} at room temperature (Figure 4a). The adsorption equilibrium for catechol on DhaTab-PBA was reached within 40 min, indicating the fast catechol adsorption. Further analysis of the time-dependent adsorption capacity reveals that the adsorption was better fitted to the pseudo-second-order kinetics than the first-order kinetics (Figure 4b and Figure S9; Table S4).

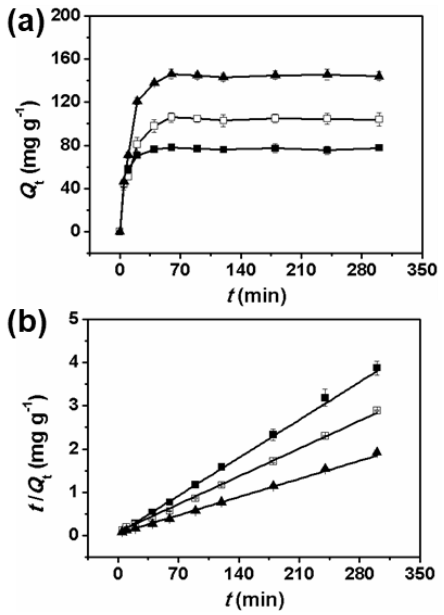

Figure 4. (a) Time-dependent adsorption for catechol on DhaTab-PBA at room temperature. (b) Plots of the pseudo-second-order kinetics for the catechol adsorption. (■) 0.025, (□) 0.050, and (▲) 0.075 mg mL^{-1}.

3.3. Effects of pH and ionic strength on the adsorption of catechol. An appropriate pH is crucial to the recognition interaction between phenylboronic acid and cis-diols, depending on the dissociation constant (pKa) of phenylboronic acid molecule and cis-diol molecule.[47] Therefore, the effect of pH on the catechol adsorption was tested in a pH range of 3-10. The adsorption capacity for catechol on DhaTab-PBA obviously increased with pH in the range of 3-7, and remained almost constant from pH 7 to pH 10 (Figure S10a). The increasing dissociated 4-MPBA (pKa = 6.2, 298 K) over pH 6 is favorable for the formation of stable five/six-membered cyclic esters. Meanwhile, the un-dissociated catechol (pKa = 9.5, 298 K) at pH < 10 is favorable for the recognition of phenylboronic acid moiety. The variation of NaCl concentration in a range of 0-0.3 mol L^{-1} gave no significant effect on the adsorption capacity for catechol on DhaTab-PBA (Figure S11). Therefore, further study was performed at pH 8 in the absence of salt.

3.4. Adsorption isotherms for catechol. Adsorption experiments were carried out in an initial concentration range of 0.02-0.10 mg mL^{-1} catechol solution at different temperature for 60 min to evaluate the adsorption isotherms for catechol on DhaTab-PBA (Figure 5a). The adsorption capacity for catechol increased in the range of 0.02-0.05 mg mL^{-1} and then levelled off with further increase of the initial catechol concentration. The adsorption isotherms could be well described with the Langmuir equation (Figure 5b):

$$\frac{C_e}{Q_e} = \frac{1}{bQ_{max}} + \frac{C_e}{Q_{max}} \quad (1)$$

where C_e (mg mL^{-1}), Q_e (mg g^{-1}) and Q_{max} (mg g^{-1}) are the concentration of catechol in solution at equilibrium, the experimental adsorption capacity at equilibrium and the theoretical maximal adsorption capacity, respectively, b (mL mg^{-1}) represents the Langmuir constant.

The Langmuir constant *(b*) and the maximum adsorption capacity (Q_{max}) were determined by plotting C_e/Q_e against C_e (Figure S14). The Q_{max} for catechol on DhaTab-PBA was 160.0 mg g^{-1}, obviously higher than that of DhaTab-V (89.3 mg g^{-1}) at room temperature (Figure S12; Table S5). The result shows that the introduction of phenylboronic acid moiety into the COF significantly enhanced the adsorption of catechol.

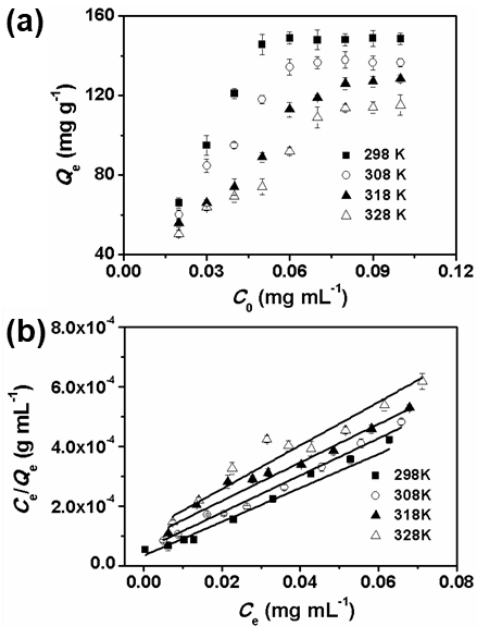

Figure 5. (a) Adsorption isotherms for catechol adsorption on DhaTab-PBA in the range of 298-328 K. (b) The corresponding Langmuir plots in the range of 298-328 K.

To further study the adsorption behaviour of DhaTab-PBA, the adsorption isotherms were investigated in the temperature range of 298-328 K (Figure 5; Table S6). Free energy change (ΔG, kJ mol^{-1}), entropy change (ΔS, J mol^{-1} K^{-1}), enthalpy change (ΔH, kJ mol^{-1}), and the thermodynamic equilibrium constant (K_0) were calculated on the basis of eqs 2-4:

$$K_0 = \frac{Q_e}{C_e} \quad (2)$$

$$\Delta G = -RT \ln K_0 \quad (3)$$

$$\ln K_0 = \frac{\Delta S}{R} - \frac{\Delta H}{RT} \quad (4)$$

where R is the universal gas constant (8.314 J mol^{-1} K^{-1}). ln K_0 was obtained from the intercept by plotting ln (Q_e/C_e) versus Q_e, while ΔH and ΔS were obtained from the plot of ln K_0 versus 1/T (Figure S13).

Table S7 shows the determined ΔG, ΔH and ΔS for the adsorption of catechol on DhaTab-PBA. The results suggest that the adsorption of catechol on DhaTab-PBA is thermodynamically spontaneous (negative ΔG) with exothermic (negative ΔH) and random-decreased (negative ΔS) process. Therefore, the efficient catechol adsorption on DhaTab-PBA was controlled by the negative enthalpy change.

3.5. Adsorption selectivity. Other types of compounds (resorcinol, hydroquinone, phenol, toluene, chlorobenzene and aniline) with similar chemical structures to cis-diols catechol were chosen as competitors to evaluate the selectivity of DhaTab-PBA (Figures S14 and S15). DhaTab-PBA was much more selective for the adsorption of catechol (Q_e = 152.6 mg g^{-1}) than other competitors (Q_e = 73.7-84.5 mg g^{-1}) (Figure S15). However, DhaTab-V showed similar adsorption capacity for catechol and competitors in the range of 79.0-84.4 mg g^{-1} (Figure S15). The results indicate that the recognition of phenylboronic acid moiety in addition to π-π interaction resulted in the higher adsorption capacity for catechol on DhaTab-PBA.

3.6. Desorption of catechol from DhaTab-PBA. In view of green chemistry and practical application, an appropriate desorption condition is vital to the regeneration of the sorbent. Hence, the effect of the type of eluent, pH and elution time on the desorption of catechol from DhaTab-PBA were tested in views of the recognition of phenylboronic acid and π-π interaction. The results show that the adsorbed catechol was effectively desorbed from DhaTab-PBA with PBS (pH 3, 1 mL, 10 mmol L^{-1}) in combination with ethanol (1 mL) for 3 min (Figure S16).

3.7. Reusability. The adsorption capacity for catechol on the regenerated DhaTab-PBA was examined to reveal the reusability of DhaTab-PBA. No obvious loss in the adsorption capacity for catechol was observed within five cycles of adsorption-desorption (Q_e = 145.4 mg g^{-1} $\pm$ 2.4,

n=5) (Figure S17), indicating good reusability of DhaTab-PBA for catechol removal from aqueous solution. Five adsorption-desorption cycles led to a slight decrease in the crystallinity and surface area of DhaTab-PBA, but no obvious change in the pore volume and the zeta potential display, indicating the good stability of DhaTab-PBA (Figure S18).

3.8. Comparison with other sorbents. In comparison with DhaTab-V, DhaTab-PBA shows a significant improvement in adsorption capacity and selectivity for catechol (Figure 6a, Figure S12 and S19, Table S5), indicating the necessity and effectiveness for the introduction of phenylboronic acid to COF. Though the introduction of phenylboronic acid moiety on COF caused the reduction of surface areas and total pore volume, DhaTab-PBA still had higher adsorption capacity for catechol than DhaTab-V due to the high affinity of DhaTab-PBA to catechol from the selective recognition of the phenylboronic acid for catechol. In comparison with the other previous sorbents for catechol, DhaTab-PBA gave 1.1-4.6 times larger adsorption capacity (Table S8). Moreover, DhaTab-PBA showed faster adsorption kinetics than previous adsorbents except hydroxyl-containing gemini surfactants modified montmorillonite (Table S8).

3.9. Adsorption capacity for catechol in environmental water. To evaluate the feasibility of DhaTab-PBA in practical application, we used it as the sorbent to remove catechol from tap water, lake and river water samples. The experimental maximum adsorption capacity (Q'_{max}) for catechol on DhaTab-PBA in real water samples ranged from 133.3 mg g^{-1} to 151.5 mg g^{-1}, comparable with Q_{max} (160.0 mg g^{-1}) in the standard catechol solution (Table S9). The results reveal that DhaTab-PBA is a feasible and potential sorbent for catechol removal from environmental water.

4. CONCLUSIONS

In summary, we have reported a thiol-ene click strategy for the preparation of phenylboronic acid-functionalized COF (DhaTab-PBA) for catechol removal from aqueous solution. The recognition of phenylboronic acid, π-π interaction and porous COF structure make DhaTab-PBA promising for the removal of catechol from environmental water with large adsorption capacity, and good adsorption selectivity and reusability.

ASSOCIATED CONTENT

Supporting Information

The Supporting Information is available free of charge on the ACS Publications website at DOI: Supplementary methods, figures and tables as mentioned in the text (PDF).

AUTHOR INFORMATION

Corresponding Author

* E-mail: xpyan@jiangnan.edu.cn

ORCID

Shi-lei Ji: 0000-0003-2250-6187

Hai-Long Qian: 0000-0001-7554-4115

Cheng-Xiong Yang: 0000-0002-0817-2232

Xu Zhao: 0000-0001-8000-9045

Xiu-Ping Yan: 0000-0001-9953-7681

Notes

There is no conflict to declare.

ACKNOWLEDGMENT

This work was supported by the National Natural Science Foundation of China (Nos. 21775056 and 21777074) and the National First-class Discipline Program of Food Science and Technology (No. JUFSTR20180301).

REFERENCES

(1) Dellinger B.; Pryor W. A.; Cueto R.; Squadrito G. L.; Hegde V.; Deutsch W. A. Role of Free Radicals in the Toxicity of Airborne Fine Particulate Matter. *Chem. Res. Toxicol.* **2001**, *14*, 1371-1377.

(2) Huang J. H.; Huang K. L.; Yan C. Application of an Easily Water-Compatible Hypercrosslinked Polymeric Adsorbent for Efficient Removal of Catechol and Resorcinol in Aqueous Solution. *J. Hazard. Mater.* **2009**, *167*, 69-74.

(3) Phutdhawong W.; Chowwanapoonpohn S.; Buddhasukh D. Electrocoagulation and Subsequent Recovery Phenolic Compounds. *Anal. Sci.* **2000**, *16*, 1083-1084.

(4) Kaleta J. Removal of Phenol from Aqueous Solution by Adsorption. *Can. J. Civil Eng.* **2006**, *33*, 546-551.

(5) Özkaya B. Adsorption and Desorption of Phenol on Activated Carbon and a Comparison of Isotherm Models. *J. Hazard. Mater.* **2006**, *129*, 158-163.

(6) Jiang Y. M.; Jia L. P.; Yu S. J.; Wang C. M. An In-ZnO Nanosheet-Modified Carbon Nanotube-Polyimide Film Sensor for Catechol Detection. *J. Mater. Chem. A* **2014**, *2*, 6656-6662.

(7) Liu Y. N.; Gao M. L.; Gu Z.; Luo Z. X.; Ye Y. G.; Lu L. F. Comparison between the Removal of Phenol and Catechol by Modified Montmorillonite with Two Novel Hydroxyl-Containing Gemini Surfactants. *J. Hazard. Mater.* **2014**, *267*, 71-80.

(8) Erogul S.; Bas S. Z.; Ozmen M.; Yildiz S. A New Electrochemical Sensor Based on Fe_3O_4 Functionalized Graphene Oxide-Gold Nanoparticle Composite Film for Simultaneous Determination of Catechol and Hydroquinone. *Electrochim. Acta* **2015**, *186*, 302-313.

(9) Chen Y.; Liu X.; Zhang S.; Yang L.; Liu M.; Zhang Y.; Yao S. Ultrasensitive and Simultaneous Detection of Hydroquinone, Catechol and Resorcinol Based on the

Electrochemical co-Reduction Prepared Au-Pd Nanoflower/Reduced Graphene Oxide Nanocomposite. *Electrochim. Acta* **2017**, *231*, 677-685.

(10) Sun Y.; Chen J. L.; Li A. M.; Liu F. Q.; Zhang Q. X. Adsorption of Resorcinol and Catechol from Aqueous Solution by Aminated Hypercrosslinked Polymers. *React. Funct. Polym.* **2005**, *64*, 63-73.

(11) Deosarkar S. P.; Pangarkar V. G. Adsorptive Separation and Recovery of Organics from PHBA and SA Plant Effluents. *Sep. Purif. Technol.* **2004**, *38*, 241-254.

(12) Körbahti B. K.; Aktas N.; Tanyolaç A. Optimization of Electrochemical Treatment of Industrial Paint Wastewater with Response Surface Methodology. *J. Hazard. Mater.* **2007**, *148*, 83-90.

(13) Marini M.; Pourabbas B.; Pilati F.; Fabbri P. Functionally Modified Core-Shell Silica Nanoparticles by One-Pot Synthesis. *Colloids Surf. A* **2008**, *317*, 473-481.

(14) Li H. T.; Xu M. C.; Shi Z. Q.; He B. L. Isotherm Analysis of Phenol Adsorption on Polymeric Adsorbents Nonaqueous Solution. *J. Colloid Interface Sci.* **2004**, *271*, 47-54.

(15) Nevskaia D. M.; Lopez E. C.; Munoz V.; Ruiz A. G. Adsorption of Aromatic Compounds from Water by Treated Carbon Materials. *Environ. Sci. Technol.* **2004**, *38*, 5786-5796.

(16) László K.; Podkościelny P.; Dąbrowski A. Heterogeneity of Activated Carbons with Different Surface Chemistry in Adsorption of Phenol from Aqueous Solutions. *Appl. Surf. Sci.* **2006**, *252*, 5752-5762.

(17) Ahmaruzzaman M. Adsorption of Phenolic Compounds on Low-Cost Adsorbents: A Review. *Adv. Colloid Interface Sci.* **2008**, *143*, 48-67.

(18) Cote A. P.; Benin A. I.; Ockwig N. W.; O'Keeffe M.; Matzger A. J.; Yaghi O. M. Porous, Crystalline, Covalent Organic Frameworks. *Science* **2005**, *310*, 1166-1170.

(19) Zwaneveld N. A. A.; Pawlak R.; Abel M.; Catalin D.; Gigmes D.; Bertin D.; Porte L. Organized Formation of 2D Extended Covalent Organic Frameworks at Surfaces. *J. Am. Chem. Soc.* **2008**, *130*, 6678-6679.

(20) Ding S. Y.; Wang W. Covalent Organic Frameworks (COFs): from Design to Applications. *Chem. Soc. Rev.* **2013**, *42*, 548-568.

(21) Kandambeth S.; Venkatesh V; Shinde D. B.; Kumari S.; Halder A.; Verma S.; Banerjee R. Self-Templated Chemically Stable Hollow Spherical Covalent Organic Framework. *Nature Commun.* **2016**, *6*, 6786.

(22) Qian H. L.; Yang C. X.; Wang W. L.; Yang C.; Yan X. P. Advances in Covalent Organic Frameworks in Separation Science. *J. Chromatogr. A* **2018**, *1542*, 1-18.

(23) Yang C. X.; Liu C.; Cao Y. M.; Yan X. P. Facile Room-Temperature Solution-Phase Synthesis of a Spherical Covalent Organic Framework for High-Resolution Chromatographic Separation. *Chem. Commun.* **2015**, *51*, 12254-12257.

(24) Li Y.; Yang C. Y.; Yan X. P. Controllable Preparation of Core-Shell Magnetic Covalent-O rganic Framework Nanospheres for Efficient Adsorption and Removal of Bisphenols in Aqueous Solution. *Chem. Commun.* **2017**, *53*, 2511-2514.

(25) Liu Z. S.; Wang H. W.; Ou J. J.; Chen L. F.; Ye M. L. Construction of Hierarchically Porous Monoliths from Covalent Organic Frameworks (COFs) and their Application for Bisphenol A Removal. *J. Hazard. Mater.* **2018**, *355*, 145-153.

(26) Yan Z.; Hu B.; Li Q.; Zhang S.; Pang J.; Wu C. Facile Synthesis of Covalent Organic Framework Incorporated Electrospun Nanofiber and Application to Pipette Tip Solid Phase Extraction of Sulfonamides in Meat Samples. *J. Chromatogr. A* **2019**, *1584*, 33-41.

(27) Guo J. X.; Qian H. L.; Zhao X.; Yang C.; Yan X. P. In Situ Room-Temperature Fabrication of a Covalent Organic Framework and its Bonded Fiber for Solid-Phase Microextraction of Polychlorinated Biphenyls in Aquatic Products. *J. Mater. Chem. A* **2019**, *7*, 13249-13255.

(28) Ding S. Y.; Gao J.; Wang Q.; Zhang Y.; Song W. G.; Su C. Y.; Wang W. Construction of Covalent Organic Framework for Catalysis: Pd/COF-LZU1 in Suzuki-Miyaura Coupling Reaction. *J. Am. Chem. Soc.* **2011**, *133*, 19816-19822.

(29) Xu H.; Gao J.; Jiang D. L. Stable, Crystalline, Porous, Covalent Organic Frameworks as a Platform for Chiral Organocatalysts. *Nat. Chem.* **2015**, *7*, 905-912.

(30) Wang X. R.; Han X.; Zhang J.; Wu X. W.; Liu Y.; Cui Y. Homochiral 2D Porous Covalent Organic Frameworks for Heterogeneous Asymmetric Catalysis. *J. Am. Chem. Soc.* **2016**, *138*, 12332-12335.

(31) Han S. S.; Furukawa H.; Yaghi O. M.; Goddard III W. A. Covalent Organic Frameworks as Exceptional Hydrogen Storage Materials. *J. Am. Chem. Soc.* **2008**, *130*, 11580-11581.

(32) Doonan C. J.; Tranchemontagne D. J.; Glover T. G.; Hunt J. R.; Yaghi O. M. Exceptional Ammonia Uptake by a Covalent Organic Framework. *Nat. Chem.* **2010**, *2*, 235-238.

(33) Fan H. W.; Mundstock A.; Feldhoff A.; Knebel A.; Gu J. H.; Meng H.; Caro J. Covalent Organic Framework-Covalent Organic Framework Bilayer Membranes for Highly Selective Gas Separati*on. J. Am. Chem. Soc.* **2018**, *140*, 10094-10098.

(34) Wang S.; Wang Q. Y.; Shao P. P.; Han Y. Z.; Gao X.; Ma L.; Yuan S.; Ma X. J.; Zhou J. W.; Feng X.; Wang B. Exfoliation of Covalent Organic Frameworks into Few-Layer Redox-Active Nanosheets as Cathode Materials for Lithium-Ion Batteries. *J. Am. Chem. Soc.* **2017**, *139*, 4258-4261.

(35) Qian H. L.; Dai C.; Yang C. X.; Yan X. P. High-Crystallinity Covalent Organic Framework with Dual Fluorescence Emissions and Its Ratiometric Sensing Application. *ACS Appl. Mater. Interfaces* **2017**, *9*, 24999-25005.

(36) Zhang X.; Chi K. N.; Li D. L.; Deng Y.; Ma Y. C.; Xu Q. Q.; Hu R.; Yang Y. H. 2D-Porphrinic Covalent Organic Framework-Based Aptasensor with Enhanced Photoelectrochemical Response for the Detection of C-reactive Protein. *Biosens. Bioelectron.* **2019**, *129*, 64-71.

(37) Merí-Bofí L.; Royuela S.; Zamora F.; Ruiz-González M. L.; Segura J. L.; Muñoz-Olivas R.; Mancheño M. J. Thiol Grafted Imine-Based Covalent Organic Frameworks for Water Remediation through Selective Removal of Hg(II). *J. Mater. Chem. A* **2017**, *5*, 17973-17981.

(38) Lohse M. S.; Stassin T.; Naudin G.; Wuttke S.; Ameloot R.; Vos D. D.; Medina D. D.; Bein T. Sequential Pore Wall Modification in a Covalent Organic Framework for Application in Lactic Acid Adsorption. *Chem. Mater.* **2016**, *28*, 626-631.

(39) Sun Q.; Aguila B.; Perman J.; Earl L. D.; Abney C. W.; Cheng Y. C.; Wei H.; Nguyen N.; Wojtas L.; Ma S. Q. Postsynthetically Modified Covalent Organic Frameworks for Efficient and Effective Mercury Removal. *J. Am. Chem. Soc.* **2017**, *139*, 2786-2793.

(40) Lu Q. Y.; Ma Y. C.; Li H.; Guan X. Y.; Yusran Y.; Xue M.; Fang Q. R.; Yan Y. S.; Qiu S. L.; Valtchev V. Postsynthetic Functionalization of Three-Dimensional Covalent Organic

Frameworks for Selective Extraction of Lanthanide Ions. *Angew. Chem. Int. Ed.* **2018**, *57*, 6042-6048.

(41) Ji W. H.; Guo Y. S.; Wang X.; Lu X. F.; Guo D. S. Amino-modified Covalent Organic Frameworks as Solid Phase Extraction Adsorbent for Determination of Carboxylic Acid Pesticides in Environmental Water Samples. *J. Chromatogr. A* **2019**, *1595*, 11-18.

(42) Hu K.; Lv Y. X.; Ye F. G.; Chen T.; Zhao S. L. Boric-Acid-Functionalized Covalent Organic Framework for Specific Enrichment and Direct Detection of cis-Diol-Containing Compounds by Matrix-Assisted Laser Desorption/Ionization Time-of-Flight Mass Spectrometry. *Anal. Chem.* **2019**, *91*, 6353-6362.

(43) Li Y.; Yang C.-X.; Qian H.-L.; Zhao X.; Yan X.-P. Carboxyl-Functionalized Covalent Organic Frameworks for the Adsorption and Removal of Triphenylmethane Dyes. *ACS Appl. Nano Mater.* 2019, doi.org/10.1021/acsanm.9b01781.

(44) Fernandes S. P. S.; Romero V.; Espiña B.; Salonen L. M. Tailoring Covalent Organic Frameworks to Capture Water Contaminants. *Chem. Eur. J.* **2019**, *25*, 1-14.

(45) Ding S. Y.; Dong M.; Wang Y. W.; Chen Y. T.; Wang H. Z.; Su C. Y.; Wang W. Thioether-Based Fluorescent Covalent Organic Framework for Selective Detection and Facile Removal of Mercury(II). *J. Am. Chem. Soc.* **2016**, *138*, 3031-3037.

(46) Enomoto I.; Soeda S.; Nakamura, I.; Yamaguchi, K. Immobilization of Dyeing Sites to Polyethylene by Plasma Treatment. *J. Photopolym. Sci. Technol.* **2013**, *26*, 539-544.

(47) Mader H. S.; Wolfbeis O. S. Boronic Acid Based Probes for Macrodetermination of Saccharides and Glycosylated Biomolecules. *Microchimica Acta* **2008**, *162*, 1-34.

For Table of Contents Only